Received: 20 January 2017 | Revised: 3 May 2017 | Accepted: 18 May 2017

DOI: 10.1002/jat.3498

WILEY Journal of Applied Toxicology

RESEARCH ARTICLE

Untargeted metabolomics of neuronal cell culture: A model system for the toxicity testing of insecticide chemical exposure

Sarah Hayton[1,2] | Garth L. Maker[1,2] | Ian Mullaney[2] | Robert D. Trengove[1]

[1] Separation Sciences and Metabolomics Laboratories, Murdoch University, Perth, WA, Australia

[2] School of Veterinary and Life Sciences, Murdoch University, Perth, WA, Australia

Correspondence
Dr. Garth L Maker, Medical and Molecular Sciences, School of Veterinary and Life Sciences, Murdoch University, South Street, Murdoch 6150, Western Australia
Email: g.maker@murdoch.edu.au

Funding information
Australian Government Research Training Program Scholarship; McCusker Charitable Foundation; National Collaborative Research Infrastructure Strategy Bioplatforms Australia

Abstract

Toxicity testing is essential for the protection of human health from exposure to toxic environmental chemicals. As traditional toxicity testing is carried out using animal models, mammalian cell culture models are becoming an increasingly attractive alternative to animal testing. Combining the use of mammalian cell culture models with screening-style molecular profiling technologies, such as metabolomics, can uncover previously unknown biochemical bases of toxicity. We have used a mass spectrometry-based untargeted metabolomics approach to characterize for the first time the changes in the metabolome of the B50 cell line, an immortalised rat neuronal cell line, following acute exposure to two known neurotoxic chemicals that are common environmental contaminants; the pyrethroid insecticide permethrin and the organophosphate insecticide malathion. B50 cells were exposed to either the dosing vehicle (methanol) or an acute dose of either permethrin or malathion for 6 and 24 hours. Intracellular metabolites were profiled by gas chromatography–mass spectrometry. Using principal components analysis, we selected the key metabolites whose abundance was altered by chemical exposure. By considering the major fold changes in abundance (>2.0 or <0.5 from control) across these metabolites, we were able to elucidate important cellular events associated with toxic exposure including disrupted energy metabolism and attempted protective mechanisms from excitotoxicity. Our findings illustrate the ability of mammalian cell culture metabolomics to detect finer metabolic effects of acute exposure to known toxic chemicals, and validate the need for further development of this process in the application of trace-level dose and chronic toxicity studies, and toxicity testing of unknown chemicals.

KEYWORDS

B50 cell line, GC–MS, Malathion, metabolomics, neurotoxicity, Permethrin

1 | INTRODUCTION

Insecticides have been used across the globe for several decades as the forefront of efforts to control pest species that threaten agriculture, animal or human health. The use of insecticides has allowed for greater human access to farmed food, strengthened agricultural economies and prevented outbreaks in vector-borne diseases such as malaria (Curtis & Mnzava, 2000; Hemingway, 2014). As the use of insecticides is widespread, and knowledge of their persistence in the environment is uncovered, there is growing concern about their use and the implications of human exposure (Fragar, Sankaran, & Thomas, 2005). Insecticide chemicals are known neurotoxins and elicit their effects on the target species by targeting features of the insect nervous system. Unfortunately, there are many features of the nervous system that are conserved across all animal species, and so insecticides can exert their toxic effects on non-target species (Keifer & Firestone, 2007).

Human exposure to insecticides has been associated with a range of neuronal health concerns, such as the prevalence of Alzheimer's disease (Welsh-Bohmer, Plassman, & Hayden, 2010; Zaganas et al., 2013), Parkinson's disease (Ascherio et al., 2006; Moretto & Colosio, 2011) and in childhood brain tumours (Searles Nielson et al., 2010), neurodevelopment (Lee, Eriksson, Fredriksson, Buratovic, & Viberg, 2015) and associated disorders such as attention-deficit-hyperactivity disorder and autism spectrum disorders (Bouchard, Bellinger, Wright, & Weisskopf, 2010; Flaskos, 2012; Liu & Schelar, 2012; Roberts et al., 2007; Timofeeva & Levin, 2010). Many insecticide chemicals are lipophilic, meaning they can accumulate within fat stores in the body and have access to the nervous system by crossing the blood–

brain barrier (Egan, 1966; Kohlmeier & Kohlmeier, 1995; Maroni, Colosio, Ferioli, & Fait, 2000). A number of recent studies have investigated the presence of insecticides and their metabolites in young children from both rural and urban areas in the United States, Europe and Australia (Babina, Dollard, Pilotto, & Edwards, 2012; Becker et al., 2006; Fenske, Lu, Barr, & Needham, 2002; Heudorf, Angerer, & Drexler, 2004; Lu, Barr, Pearson, Walker, & Bravo, 2009; Naeher et al., 2010), indicating not only the widespread exposure of insecticides and their potential for bioaccumulation, but also their potential bioavailability during key stages of development in children.

Current knowledge of the long-term human toxicity of insecticides tends to focus on the physiological end-points of exposure, often making assumptions by association. Despite the varied, specific molecular targets of the different insecticide chemical classes, the overall intended effect of insecticides on the cells of the nervous system is the same: the initial overstimulation and excitation of neuronal cells, resulting in cell exhaustion, degeneration and death (Marrs, 2012; Narahashi, 2010). The specific molecular targets or mechanisms of toxic action are well known throughout the many different classes of insecticide chemicals, as they have been elucidated from traditional toxicity testing on animals and through the development of new chemical compounds that are similar in structure and thus have the same targets as their parent compound (Stenersen, 2004). What remains unknown about the toxicity of insecticides are the immediate metabolic effects of these chemicals on the processes that occur inside neuronal cells, and what these might mean for the prolonged health of the cell and thus the nervous system. Understanding these small metabolic perturbations in neuronal cells that survive a toxic insult could potentially uncover some of the specific biochemical processes that may be responsible for the adverse effects on human health associated with insecticide chemical exposure.

Metabolite profiling (metabolomics/metabonomics) provides unique insights into the metabolic pathways of cells via the simultaneous, untargeted analysis of the small molecules (or metabolites) within a biological sample. Metabolomics has been widely applied in the field of toxicology, mainly in the context of animal studies and the analysis of urine or plasma for the discovery of biomarkers of toxic chemical exposure (Bouhifd, Hartung, Hogberg, Kleensang, & Zhao, 2013; Ramirez et al., 2013). There are studies that have utilized mammalian cell culture metabolomics to look specifically at the metabolic effects of toxic chemical exposure (Ellis et al., 2011; Huang et al., 2012; Johnson, Patterson, Idle, & Gonzalez, 2012; Snouber et al., 2013; Van den Hof et al., 2015), only a handful of these have specifically investigated neurotoxicity (Zurich & Monnet-Tschudi, 2009) including exposure to thalidomide (Qin et al., 2012), methyl-mercury and caffeine (van Vliet et al., 2008). There is clearly great potential in the application of mammalian cell culture metabolomics in the study of insecticide toxicology, and metabolomics has been suggested to be an important technique in the development of new, safer pesticide chemicals (Aliferis & Chrysayi-Tokousbalides, 2011).

The B50 neuroblastoma cell line was derived from the rat neonatal central nervous system and is in wide use today in studies of central nervous system neurons in culture (Otey, Boukhelifa, & Maness, 2003). B50 cells have been used extensively to study neuronal cell death and neurotoxicity, and are very simple to grow, making them an ideal model to investigate the potential of metabolomics in the assessment of neurotoxicity. Before any cell line model can be used as a screening test for chemicals of unknown toxicity, it first has to be validated with chemicals of known toxic effect. In this study, we used gas chromatography–mass spectrometry (GC–MS)-based untargeted metabolomics to characterize the effects to the intracellular metabolome of the B50 neuronal cell line after 6 and 24 hours of acute exposure to two known neurotoxic chemicals: the pyrethroid insecticide permethrin (Soderlund, 2012) and the organophosphate insecticide malathion (Flaskos, 2012). Cell photographs were captured to compare the metabolic response to any change in gross cell morphology. In particular, the main aim of this study was in showing that this metabolomics approach was able to identify significant fold changes in the metabolite profile of cultured mammalian neuronal cells following insult from a known toxic chemical. In addition, this study was also able to demonstrate how exposure to different classes of insecticides corresponded to distinctly different metabolite responses from the same cell line.

2 | MATERIALS AND METHODS

2.1 | Cell culture

The adherent, rat neuroblastoma cell line B50 obtained from the European Collection of Cell Cultures was grown and maintained in Dulbecco's modified eagle medium supplemented with 1% *v*/v 2 mM L-glutamine, 1% *v*/v 10 000 U ml^{-1} combined penicillin and streptomycin, and 5% *v*/v foetal calf serum. Cells were kept in a humidified incubator at 37°C and 5% CO_2. Routine cell culture of adherent cell populations was performed in 75 cm^2 tissue culture flasks with 10 ml volume of medium during the growth phase. Medium was replaced after 48–72 hours of initial seeding, when the phenol red indicator in the medium showed a drop in pH. For passaging confluent cells and cell counting during experimentation, cells were detached with addition of 0.25% trypsin–EDTA solution (2.5 g porcine trypsin and 0.2 g EDTA per litre) after first removing the medium and washing the cells with pre-warmed 1× phosphate-buffered saline (PBS). Cell culture passage numbers 28–32 were used for experimentation. The cells were tested using PCR for mycoplasma status along with the HGH housekeeping gene and were found to be negative for the presence of mycoplasma. All cell culture solutions and PBS were purchased from Sigma-Aldrich (Castle Hill, NSW, Australia).

2.2 | Experimental design

For analysis of the metabolome, cells were cultivated in six-well tissue culture plates and seeded at a density of 4×10^5 cells per well in 2 ml of medium. Plates were left for 24 hours to allow for cell adhesion before being exposed to either permethrin or malathion added as a solution in 100% methanol to a final concentration in each well of 200 μg ml^{-1} (equivalent to 0.51 and 0.61 mM for permethrin and malathion, respectively). Both compounds were purchased at the highest purity available (>98%, with permethrin as an equal mixture of *cis*- and *trans*-isomers) from Sigma-Aldrich. The final concentration of methanol in the cell medium was <0.1% total volume. The same volume of methanol was added to the same number of equally prepared wells

as an unexposed vehicle control group. Control and exposure groups for both time points of one insecticide exposure were set up simultaneously using cells from the same passage number to minimize uncontrolled variables. Five wells from one 6-well plate were combined as one sample within a particular treatment group. The sixth well was used to count the cell number as a representative parallel sample to normalize data to the amount of tissue analysed. The number of biological replicates set up per treatment group was four. Following addition of either insecticide compound, both 'non-exposed' and 'exposed' treatment groups for each compound were left for 6 hours and another set for 24 hours exposure, in a humidified incubator at 37°C and 5% CO_2. Immediately preceding sampling, cell number and viability were determined for each sample using Trypan blue exclusion following trypsinization of the parallel cell number sample, by diluting 10 µl of cell suspension 1 : 2 with a 0.4% Trypan blue (Allied Chemicals, Lalor, VIC, Australia) in 1 x PBS solution and immediately counting cells using a Bright-Line Haemocytometer (Hausser Scientific, Horsham, PA, USA) and an inverted light microscope (Olympus Australia, Notting Hill, VIC, Australia). Photographs were also taken immediately before sampling (Moticam 2300; Motic China Group Co., Hong Kong) to document differences in cell density and gross morphology between the control and exposure groups. All methanol and water used in this study was liquid chromatography-MS grade purity and purchased from LabScan (Gillman, SA, Australia).

2.3 | Sampling for intracellular metabolites

For analysis of intracellular metabolites, immediately following completion of the respective exposure time, all plates of both unexposed and exposed treatment groups were removed from incubation and cellular activity halted by placing the plates directly on to ice. Culture medium was discarded and cellular metabolism immediately quenched by careful addition of 1 ml 4°C 1× PBS to each well, ensuring minimal disruption of adhered cells from the plate surface. This PBS was removed as a washing step to remove any residual medium from the cells. Adhered cells were then collected by scraping into 100 µl of additional PBS and pooling the cell suspension from five wells into one microcentrifuge tube. All collected samples were immediately snap-frozen and freeze-dried using a FreeZone Plus Cascade Benchtop Freeze Dry System (Kansas City, MO, USA) to prevent degradation or loss of metabolites (Mediani et al., 2015). Freeze-dried samples were stored at −80°C until metabolite extraction.

For extraction of intracellular metabolites, freeze-dried cell samples were resuspended in 500 µl of 100% methanol containing 2.6 µg ml^{-1} of $^{13}C_6$-sorbitol (Sigma-Aldrich), an isotopically labelled compound that is easily resolved used as an internal standard to normalize analytical data, to minimize any observed effect from extraction or instrumental variability. The suspended cells in the extraction solution were agitated in a Precellys 24 Tissue Lyser (Bertin Technologies, Aix-en-Provence, France) for 2× 20 s cycles at 6500 rpm to maximize the metabolite recovery rate. Homogenized extracts were centrifuged for 10 min at 16 100 *g* and supernatant collected into fresh microcentrifuge tubes. Pellets of cell debris were discarded. Extracted metabolites were concentrated by evaporating the methanol in a Concentrator Plus Rotary Vacuum Concentrator (Eppendorf South Pacific, Macquarie Park, NSW, Australia) and protected from degradation by addition of water and further snap-freezing and freeze-drying. Once completely dry, metabolite extracts were stored at −80°C until preparation for GC–MS analysis.

2.4 | Gas chromatography–mass spectrometry analysis

For measurement of metabolites by GC–MS, dried metabolite extracts were derivatized by methoximation and silylation to increase thermal stability and volatility of metabolite compounds. The derivatization process had been previously optimized for a range of different biological samples (Abbiss, Rawlinson, Maker, & Trengove, 2015; Abbiss et al., 2012; Ng, Ryan, Trengove, & Maker, 2012; Wenner, Maker, Dawson, Drummond, & Mullaney, 2016). Briefly, 40 µL of 20 mg ml^{-1} methoxyamine hydrochloride in pyridine was added to a dried extract and incubated at 30°C for 90 min with agitation in a Thermomixer Comfort (Eppendorf) at 1200 rpm, followed by addition of 20 µl of *N*-methyl-trimethylsilyltrifluoroacetamide and incubation at 37°C for 30 min with agitation at 300 rpm. Derivatized metabolite extracts were transferred to amber vials with 200 µl glass inserts where 5 µl of *n*-alkanes mixture solubilized in hexane (C_{10} and C_{12} at 0.625 µg ml^{-1} and C_{15}, C_{19}, C_{22}, C_{26}, C_{32} and C_{36} at 1.250 µg ml^{-1}) was added to the sample to enable calculation of a Kovát's retention index. Derivatization of samples was carried out in 'batches' to ensure that all derivatized samples were injected and analysed within 24 hours following derivatization. Methoxyamine hydrochloride, *N*-methyl-trimethylsilyltrifluoroacetamide and *n*-alkanes were purchased from Sigma-Aldrich, pyridine from Ajax Finechem (North Ryde, NSW, Australia) and hexane from LabScan, all in the highest purity available.

A total of 1 µl of each sample was injected in splitless mode into a GC for compound separation, and mass separation and detection by electron-ionization single quadrupole MS. Analysis was performed by an Agilent 6890 Series GC system with 7683 Autosampler/Injector unit, coupled to a 5973 N Series quadrupole MS (Agilent Technologies, Santa Clara, CA, USA). The injection temperature was set at 230°C with a GC column initial temperature of 70°C ramped at 1°C min^{-1} for 5 min followed by 5.63°C min^{-1} to 330°C final temperature held for 10 min. The GC column was a 30 m Factor Four fused silica capillary column VF-5MS (ID = 0.25 mm, DF = 0.25 µm) with a 10 m EZ-Guard column (Agilent Technologies) and the carrier gas was helium set to a constant flow rate of 1 ml min^{-1}. The retention time was locked to elute a standard mannitol-TMS compound at 30.6 min. The transfer line into the MS was set at 280°C and the ionisation source at 230°C. Electron ionization was set at −70 eV and the MS scan monitoring in mass range *m/z* 45–600 at a rate of 1.56 scans s^{-1}.

2.5 | Data processing and statistical analysis

Deconvolution of GC–MS data was performed using AnalyzerPro v5.2.1.6441 (SpectralWorks Ltd., Runcorn, Cheshire, UK). Manual inspection and peak alignment of the resulting peak area matrix using the retention index (RI) ladder was carried out to reduce the occurrence of misallocated peaks and thus false positives. Identification of GC–MS peaks was achieved by comparing the MS and RI with those

of reference compounds from an in-house library of standards (Separation Science and Metabolomics Laboratory, and Metabolomics Australia, Perth, WA, Australia). In addition, a number of 'unknown' metabolites were putatively annotated through comparison of the MS with those of compounds in the commercially available National Institute of Standards and Technology (NIST, Gaithersburg, MD, USA) MS library. Only those features with >80% probability match factor to the NIST MS library were annotated as such. All other features were deemed as 'Unknown' with respective retention time, RI and base-peak spectral masses to distinguish them. For the peak area matrix, features that occurred in less than 80% of all samples were removed from subsequent analyses, unless their presence was unique to a particular treatment group in >75% of replicates. All remaining peak areas were normalized to the peak area of the internal standard compound to remove variation from any differences in extraction or instrumental procedures, and then normalized to the viable cell number in the parallel sample to remove variation from the different amounts of tissue analysed. The internal standard compound, and the *n*-alkane RI markers were then removed from the peak area matrix before statistical analyses, and the total number of detected features recorded.

The process of statistical analysis was repeated as described previously for untargeted metabolomics by GC–MS (Francki, Hayton, Gummer, Rawlinson, & Trengove, 2016), and a brief outline follows. For all multivariate and univariate statistical analyses, the peak areas (X) were first transformed using the equation $\log_{10}(X + 1)$. Principal components analysis (PCA) of both the permethrin exposure and malathion exposure peak area matrices (using a maximum seven principal components, non-linear iterative partial least squares algorithm, no rotation, full cross-validation, constant weighting and mean-centred data) was conducted using The Unscrambler X v10.3 (Camo, Oslo, Norway) and assessed for any spatial grouping and separation of different treatment groups, which would indicate a change in the overall metabolite profile. Using PCA, those metabolites that most contributed to the spatial separation could be identified from the *X*-loading plots that correspond to the PCA score plots. For all univariate statistical analyses, the data were considered non-normally distributed with unequal variances for the most conservative calculation of significant differences between a relatively small number of replicates, and a two-tailed Student's *t*-test was used to determine the effects of acute exposure of permethrin or malathion on viable cell number and metabolite peak area. Statistically significant changes were considered for $P < 0.05$. Fold changes in the mean relative abundance of each metabolite feature between non-exposed and exposed groups were calculated using non-transformed, normalized peak areas. The metabolites with substantial (>2.0 or <0.5) fold changes were grouped according to compound class (if identified) and the numbers of each recorded.

3 | RESULTS

3.1 | B50 cells display distinct growth and metabolite profiles following exposure to permethrin or malathion

Immediately preceding sampling for metabolomics analysis, a parallel sample of each replicate was counted for viable cell number to correct the metabolite abundance data for any differences in the amount of tissue analysed. Figure 1 shows cell number and percentage viability as histograms to observe the gross effect of the insecticides on cell growth. The control groups ('no exposure') show that in normal growth conditions, the total cell number increased from 4.7×10^6 cells to 8.1×10^6 cells over 24 hours, an increase of 72%, which is an expected rate of growth for this cell line in ideal conditions (Otey et al., 2003). Following exposure to permethrin or malathion, the same growth rate was not observed. Interestingly, the cells exhibited a different response to each insecticide chemical. Permethrin exposure from 0 to 24 hours resulted in an 8.5% increase, while malathion exposure had a 29.8% decrease over the same time. Comparing the control to exposure groups at each time point, the number of viable cells at 6 hours was similar for all groups; only the permethrin-exposed group showed a significant 18.5% decrease from control ($P = 0.03846$), with no distinct difference in the malathion-exposed group. At 24 hours the effect of the chemical exposure on cell growth and survival became apparent, as both insecticides showed a significant decrease in viable cells from control; permethrin exposure resulted in 37.0% fewer cells

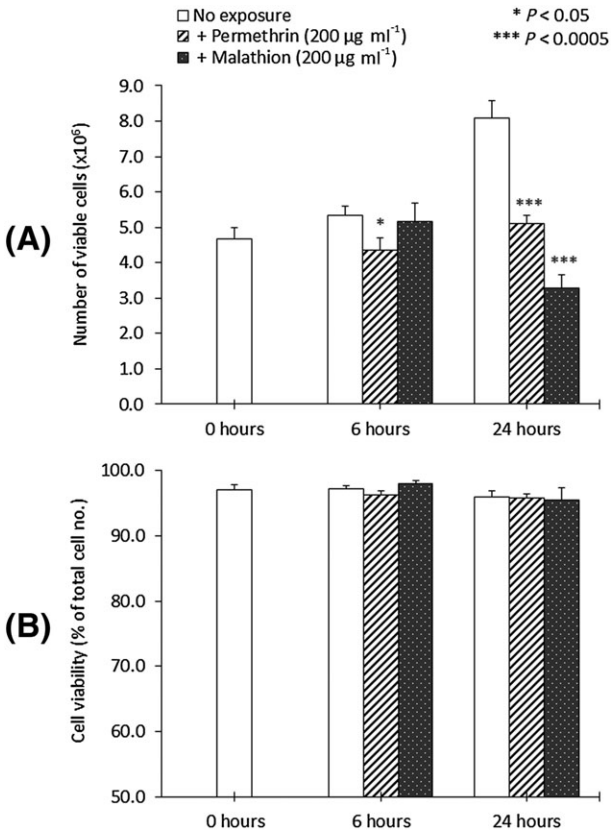

FIGURE 1 B50 cells following acute exposure to permethrin or malathion for 6 and 24 hours, counted using the Trypan blue exclusion method. A, Mean total number of viable cells ($\times 10^6$), and B, mean percentage cell viability. Control cells ('no exposure') were counted at 0 hours (time of treatment) as well as at both 6 and 24 hours and combined to obtain the overall mean. $n = 8$ for 'no exposure' group, $n = 4$ for '+Permethrin' and '+Malathion' groups. Error bars indicate 1× standard error from the mean. Significant difference in cell number to the control is shown by $^*P < 0.05$ and $^{***}P < 0.0005$. There were no observed significant differences in the percentage cell viability

than the control at the same time point (P = 0.00021), and malathion exposure caused a greater reduction, with 59.4% fewer cells ($P = 7.262 \times 10^{-6}$). The percentage of viable cells of total cell number remained the same across all groups at all time points, despite the observed reduction in cell number.

Photographs taken of all groups at 6 and 24 hours (Figure 2) are consistent with the cell number data, in that there was no marked visual difference in the cell culture of all groups at the 6 hour time point, yet at 24 hours there was a clear difference in cell number in both exposure groups compared to the control group. For both exposure groups, there not only appears to have been a change in the number of cells present, but also an altered appearance of the cells themselves, indicating that the pesticide exposure has affected morphology. Both exposure groups appeared to have a more distorted, uneven outer membrane compared to unexposed cells, and malathion-exposed cells appeared to have less extended processes, and a slightly swollen cell body, compared to permethrin exposure and the control.

To characterize the overall impact of insecticide chemical exposure on the metabolite profile, we used a pattern recognition approach based on PCA of normalized peak areas for all observable features that had >80% coverage across all samples or a unique appearance within specific treatment groups, for both sets of insecticide-exposed cells (121 and 95 intracellular metabolites total, for permethrin- and malathion-exposed profiles, respectively). A full list of these metabolites, with fold-changes from control and P values, is included in supporting information (Tables S1 and S2). As this was an untargeted investigation, features with unknown identification were also included in analysis. There were 53 features of unknown identification, and 68 features of putative identification from either the in-house mass spectral library or a high-probability match with the NIST MS database, for the permethrin exposure cell group. There were 34 unknowns, and 61 putatively identified features for the malathion exposure cell group. Figure 3 shows the PCA plots of all time points of each insecticide exposure and their control groups, and revealed that all separate groups examined produced consistently altered metabolite profiles. Further PCA was conducted to investigate the difference between control and exposure groups at each time point, and the accompanying metabolite loadings plots for each were examined for those

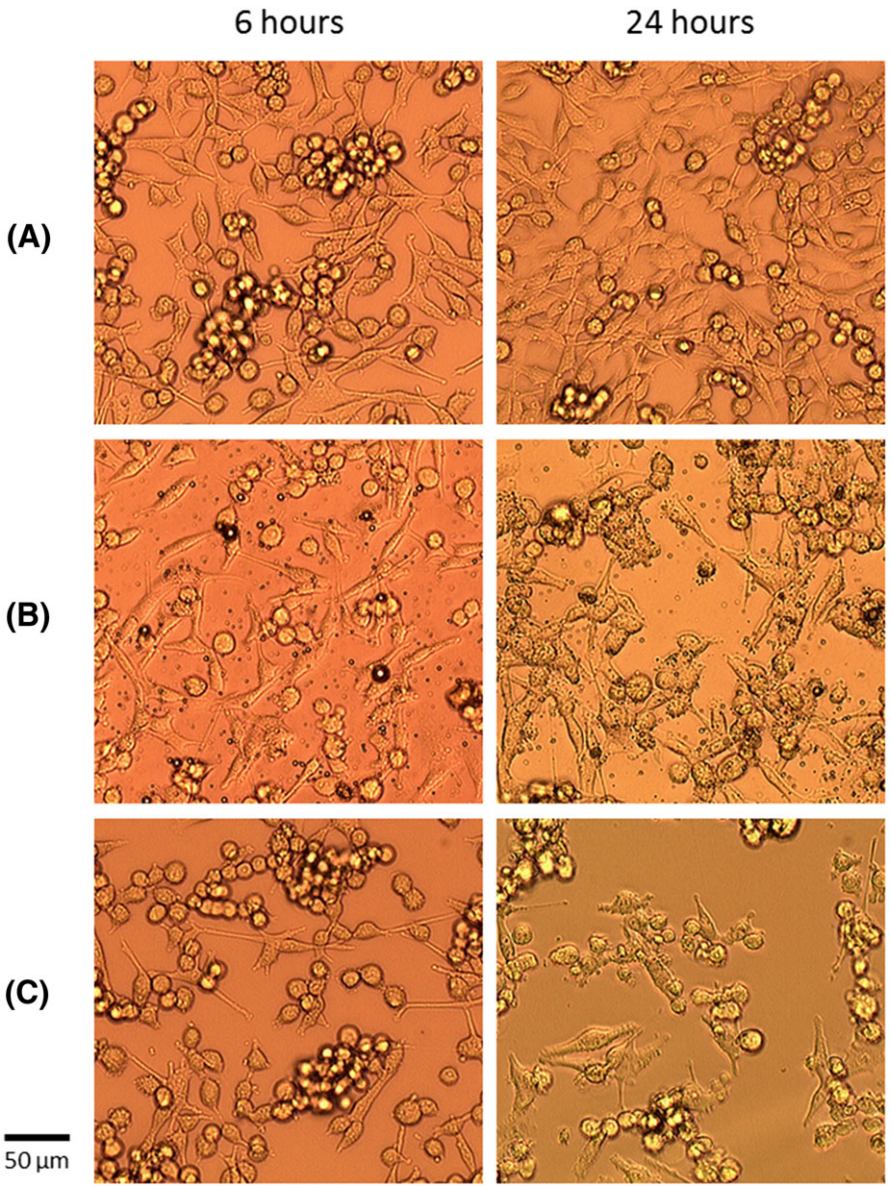

FIGURE 2 B50 cells photographed under inverted light microscope magnification. Images are of cell samples set up for metabolite profiling analysis and show cells following both 6 and 24 hours of A, no exposure (control), B, acute exposure to permethrin (200 µg ml^{-1}) and C, acute exposure to malathion (200 µg ml^{-1}). Note: due to the lowered solubility of permethrin in aqueous solution, the insolubilized portion of the insecticide formulation can be seen in the images in row B, as small particulates present in the medium

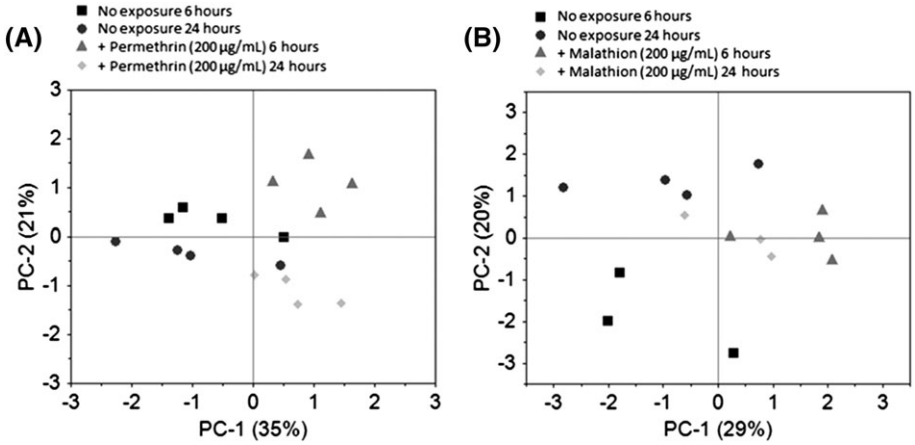

FIGURE 3 PCA scores plots showing the response of B50 cells to acute exposure of A, permethrin or B, malathion for 6 and 24 hours. PCA was applied to the intracellular metabolite profiles to assess effects of insecticide exposure. Plots show both control (no exposure) and insecticide-exposed cells for both time points. In plot A, $n = 4$ for all treatment groups. In plot B, $n = 4$ for 'No exposure 24 h' and '+Malathion 6 h' groups, and $n = 3$ for 'no exposure 6 h' and '+Malathion 24 h', due to the removal of the outlier samples. Each PCA plot was further analysed (see Supporting information, Figure S1) by separate PCA on samples from each time of exposure only, and the associated loadings plots used to investigate the metabolites that corresponded to a change in profile between control and treatment groups. PCA, principal components analysis

metabolites that contributed to the observed variation in metabolite profile (Supporting information, Figure S1).

3.2 | Analysis of principal components analysis intracellular metabolite loadings identifies metabolites associated with exposure to an insecticide chemical

From the list of metabolite loadings, the fold change in relative abundance from control was calculated as well as the *P* value (Tables S1 and S2), and only those considered a major fold change (>2.0 or <0.5) in either the 6 or 24 hour time point were selected for further interpretation in this study (75 metabolites for permethrin exposure, and 72 for malathion exposure). Figure 4 shows these fold changes as histograms of metabolites in compound classes that exhibited a different trend between the two insecticide exposures, inclusive of amino acids, fatty acids and intermediates of the tricarboxylic acid (TCA) cycle (dicarboxylic acids and pyruvate). Histograms of the remaining metabolite classes that showed substantial fold changes are included in the Supporting information (Figure S2); for carbohydrates including monosaccharides and sugar alcohols, a small number of miscellaneous metabolites inclusive of lactate and uracil, and a large number of 'unknowns'.

3.3 | Comparison of intracellular metabolite concentrations at different exposure times were distinct for two separate classes of insecticide chemical

It was observed that there was a marked difference in metabolite response of B50 cells to the different insecticides, permethrin and malathion, visualized by the fold change histograms in Figure 4. Permethrin exposure resulted in seven amino acid features that had an altered abundance considered substantially different from control levels, whereas malathion exposure resulted in 21 amino acid features whose abundance was substantially altered. The reverse trend was observed with fatty acids, where there were eight fatty acid metabolites that responded following permethrin exposure, and only two identified fatty acid metabolites that had a substantial fold change following malathion exposure. Overall, it can be observed that permethrin exposure resulted in a predominantly fatty acid-based response, whereas malathion exposure resulted in a predominantly amino acid based response.

Perhaps the most marked difference in the direction of metabolite response between the two insecticide chemical exposures was in the TCA cycle group (Figure 4); inclusive of dicarboxylic acid intermediates as well as pyruvate, all of which are important in energy synthesis for the cell. In particular, succinate and malate showed a significantly increased fold change after both 6 and 24 hour exposure to permethrin, while the opposite response occurred following malathion exposure with a significant decrease from control of the same two metabolites after the 24 hour exposure. In both cases, changes in pyruvate were opposite to that of these metabolites. Pyruvate was substantially decreased following exposure to permethrin, where the TCA cycle intermediates were increased, while with malathion exposure, pyruvate was substantially increased, where the TCA cycle intermediates were decreased.

The number of 'unknown' metabolites for both insecticide exposures was similar. There was also a differing overall response of the 'unknowns' for each metabolome (Figure S2, Supplementary information), the overall trend for permethrin exposure was a majority fold change increase from control after 24 hours of exposure, which was not seen to the same extent at 6 hours. For malathion exposure, the overall trend was a majority fold change increase from control after 6 hours of exposure, and for many of the same metabolites, this trend shifted to a decrease in fold change after 24 hours. Interestingly, there were a small number of 'unknowns' that showed enormous increased in abundance following insecticide exposure, not matched by any of the identified metabolite features. These included a 28-fold increase in one metabolite ('Unknown_40.67_2585_91, 129…'; Figure S2) after 24 hours of permethrin exposure, and four other features that had greater than fivefold increase after either 6 and/or 24 hours ('Unknown_18.27_1334_189, 292′, 'Unknown_23.39_1551_117, 170′, 'Unknown_24.04_1584_147, 334′ and 'Unknown_

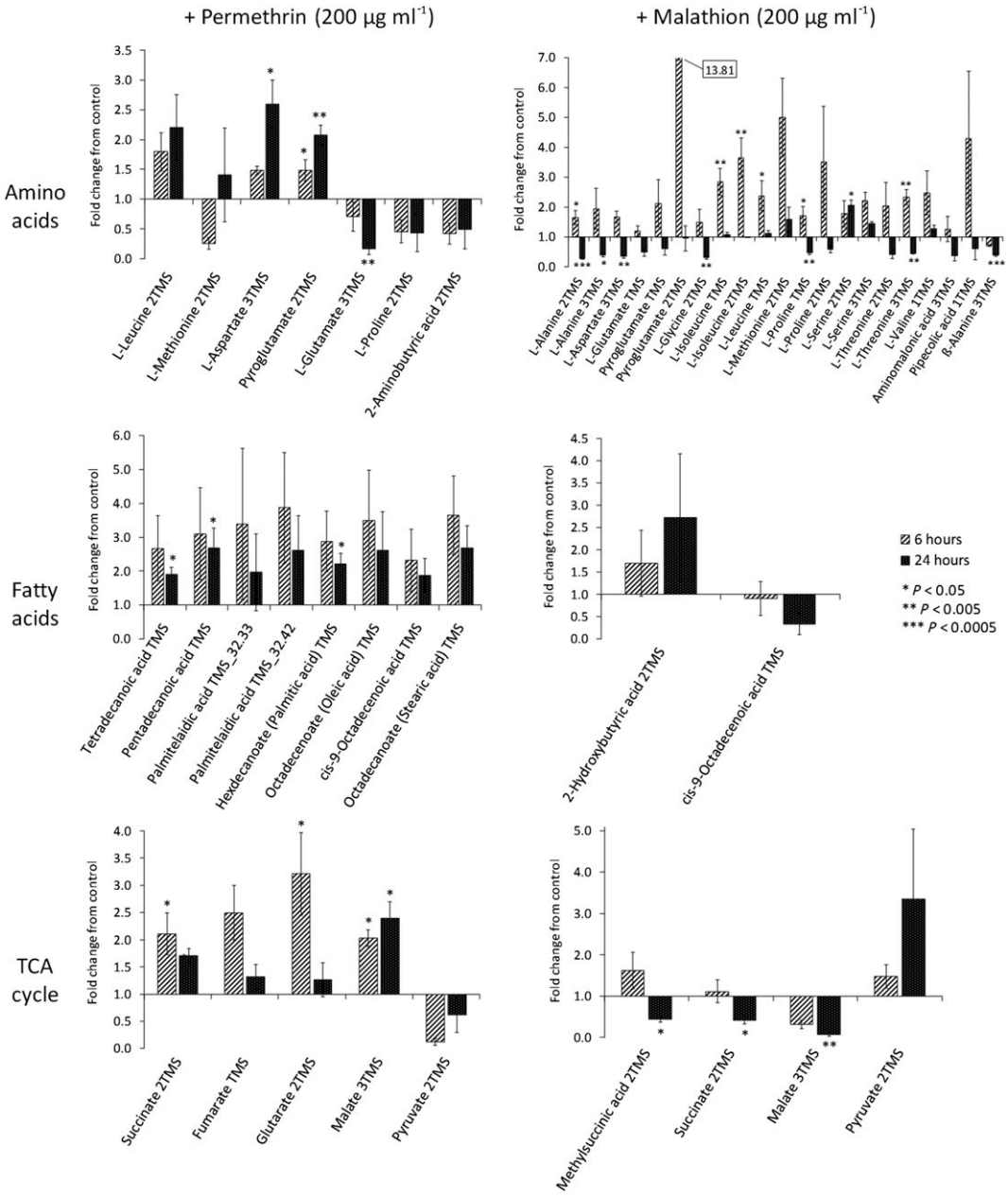

FIGURE 4 Fold change histograms showing the effect of insecticide chemical exposure on the relative abundance of intracellular metabolites that had a substantial fold change from control (>2.0 or <0.5) in the B50 cell line. Histograms show metabolites from the compound classes, amino acids, fatty acids and dicarboxylic acids and pyruvate (TCA cycle), which were measured in the metabolome after either permethrin or malathion exposure and compares fold change in abundance after 6 and 24 hours of exposure. Error bars indicate 1× standard error from the mean. Significantly different metabolite abundances in exposed cells relative to control is shown by $^{*}P < 0.05$, $^{**}P < 0.005$ and $^{***}P < 0.0005$. TCA, tricarboxylic acid; TMS, trimethylsilyl

24.58_1611_113, 198′; Figure S2). Following malathion exposure, there was one unknown feature ('Unknown_19.75_1394_147, 241, …'; Figure S2) with a 33-fold increase after 6 hours, which was not maintained at 24 hours; the same feature was still present, but with only a 2.8-fold increase. There were two other features that exhibited a vast exaggerated abundance after 6 hours of malathion exposure, at 19- and 15-fold increases ('Unknown_18.06_1325_315, 330, 147′ and 'Unknown_27,44_1755_117, 363′ respectively; Figure S2). The 'unknowns' histograms display an overall difference between the two insecticide exposures; the majority of unknown features with a substantial fold change from control showed an increased response after 24 hours of permethrin exposure that was not seen to the same extent at 6 hours, indicating a progressive response or a 'build-up' of these particular metabolites in the B50 cells. An opposite overall trend was observed for malathion exposure, where the larger, substantial fold changes occurred after 6 hours of exposure, and the response actually decreased from 6 to 24 hours, indicating a deterioration or conversion of these metabolites in B50 cells.

4 | DISCUSSION

This study has successfully observed differences in the intracellular metabolome profile of cultured neuronal B50 cells, and associated

some of the specific differences to insecticide chemical exposure. From this untargeted metabolomics analysis of cultured cells, hundreds of individual metabolite features were able to be detected (Tables S1 and S2) and a great proportion (>50%) of those contributed to a change in the metabolome following a toxic insult (Figures 4 and S2). PCAs of all samples showed that biological replicates grouped together and that specific metabolites could be distinguished for each time point of toxic exposure (Figures 3 and S1). This, together with the outcome of a large number of different classes of metabolites that were able to be detected, highlights the suitability of this cultured cell metabolomics model to monitor the cellular metabolic response to a toxic chemical exposure, and its potential for application to future toxicology testing practices. In the proposed twenty-first century model for toxicology testing and research (NRC, 2007; Ramirez et al., 2013), there are increasing demands for the use of human-derived cell lines coupled to molecular profiling platforms such as metabolomics, as a predictor for toxic adverse effects on key cellular pathways and metabolic events, not just in the advancement of current toxicology knowledge, but as an alternative to the use of animals in toxic chemical testing. One important future development would be the validation of the metabolic response in a human neuronal cell line, and the subsequent comparison to the rat B50 neuronal cell line.

Previous studies have investigated the metabolomics response in rats following exposure to different classes of pesticide chemicals, which only compared the abundance of selected 'biomarker' molecules from urine (Jones et al., 2013; Liang, Wang, Long, Li, & Wu, 2013) and serum metabolomes (Liang, Wang, Long, & Wu, 2012; Moser et al., 2015). The benefit of this cell culture metabolomics study in comparison to animal-based, 'biomarker' measurements is not only in the direct analysis of the intracellular metabolome of the cell type of interest, but also in the untargeted profiling of all detectable features that allow for the comparison of not just relative abundance, but also the quantity of substantially affected metabolites from particular classes, or of a particular pathway, that are altered from exposure to different toxic chemicals. Untargeted metabolomics is proposed to become the future direction of all metabolomics investigations (Sévin, Kuehne, Zamboni, & Sauer, 2015) and is important for the interpretation of the biological response from metabolomics data, particularly in relation to mechanistic toxicology studies and predicting potential harm from environmental chemicals (Aliferis & Chrysayi-Tokousbalides, 2011).

This study was successful in determining that a distinct response is interpretable for different chemical exposures. Metabolic changes from exposure of rats to different pesticides has been recorded by previous studies (Liang et al., 2012; Liang et al., 2013; Moser et al., 2015), although in some cases, such as permethrin exposure, the observed metabolic responses were not consistent. Liang et al. (2013) reported an increase in free amino acids in the serum of rats following long-term (60 days) exposure to permethrin. A separate study comparing the response from multiple classes of pesticide chemicals found that there was no substantial change in amino acids in rats treated with a high dose of permethrin for 2 hours (Moser et al., 2015). In this study, the response of amino acids to permethrin exposure was varied, with some increasing and others decreasing (Figure 4 and Table S1), indicating that there is some response to the pesticide exposure, but that it is not a one-way effect. The response of amino acids may be indicative of other energy metabolism processes (e.g. glycolysis or fatty acid β-oxidation) being the focus of toxic effects, and that altered usage or production of amino acids is an indirect effect. For example, this study observed that permethrin exposure had a predominantly increased fatty acid-based response in the metabolome. Permethrin, a type I pyrethroid for which the neurotoxic action involves prolonging sodium channel activation resulting in depolarization and neuronal excitotoxicity (Soderlund, 2012), is known to induce an oxidative effect within cells that leads to lipid peroxidation (Abdollahi, Ranjbar, Shadnia, Nikfar, & Rezaie, 2004; Banerjee, Seth, & Ahmed, 2001; Issam, Zohra, Monia, & Hassan, 2011).

In this study, exposure to malathion had a predominantly greater amino acid response than permethrin, evident from the number of substantial fold changes observed within the metabolite class (Figure 4). compared to that seen in permethrin exposure. Malathion, an organophosphate for which neurotoxic action is the inhibition of the enzyme acetylcholinesterase resulting in increased cholinergic signal transduction and excitotoxicity (Stenersen, 2004); it is known to elicit an excessive generation of reactive oxygen species and cause a state of oxidative stress within cells (Ojha, Yaduvanshi, Pant, Lomash, & Srivastava, 2013). However, this study suggests that malathion toxicity may also manifest via glutamate excitotoxicity, evident from the 13-fold increase in pyroglutamate following 6 hours of malathion exposure (Figure 4). Pyroglutamate is the cyclized form of glutamate, and it is known that glutamate can be freely and non-enzymatically converted to pyroglutamate under high temperature conditions, such as within an ionization source for analysis by MS (Purwaha, Silva, Hawke, Weinstein, & Lorenzi, 2014), and so levels of pyroglutamate can be considered indicative of changes in glutamate. Glutamate is the chief excitatory neurotransmitter in the mammalian nervous system and is known to be implicated in a wide variety of neurological pathologies (Choi, 1988; Tian et al., 2012; Veyrat-Durebex et al., 2016; Ward, Rego, Frenguelli, & Nicholls, 2000). Previous investigations have shown that under stressed conditions neuronal cells will have an enhanced production of glutamate (Nishizawa, 2001) and that, as a protective mechanism against glutamate-mediated excitotoxicity, cells may attempt to reduce the accumulation of glutamate by converting it into other amino acids (Wang & Qiu, 2010). The overall, substantial increase in most detectable amino acid compounds observed in this study after 6 hours of malathion exposure supports an attempted protective mechanism against glutamate-mediated excitotoxicity in response to malathion exposure. To provide mechanistic evidence for this speculation, future metabolomics studies could include cultured cells supplemented with radioisotope-labelled glutamine, as a way of tracking the directional flow through metabolic pathways of glutamine to glutamate, and the conversion into other amino acids (Mueller & Heinzle, 2013; Sims, Manteiger, & Lee, 2013).

In this study the most notable, specific difference between the two insecticide exposures was that of the TCA cycle intermediates and pyruvate (Figure 4), where both chemical exposures resulted in substantial and opposite responses from control in these metabolites, indicating that energy synthesis was disrupted in both circumstances to different extents. Pyruvate had the opposite response to the TCA cycle intermediates with both permethrin and malathion exposure. Permethrin exposure showed decreased pyruvate abundance

compared to increased TCA cycle intermediates, while malathion exposure showed an increased abundance of pyruvate compared to decreased TCA cycle intermediates. Further to the earlier suggestion of glutamate-mediated excitotoxicity in malathion-exposed cells, it may be possible that if glutamate was being converted into other amino acids as an attempted protective mechanism, this would reduce the glutamate available to power the TCA cycle (via the glutamate/glutamine cycle) (McKenna, 2007; Peng et al., 1993), and so account for the significantly decreased abundance of TCA cycle intermediates in malathion-exposed cells at 24 hours (Figure 4). A limitation to this is that an enzyme involved in the glutamate/glutamine cycle, glutamine synthetase, is specifically located in astrocytes, and not in neurons (Peng et al., 1993), implying that this is not the mechanism occurring in our neuronal cell model. The same is true for an important TCA cycle enzyme, pyruvate carboxylase, also located specifically in astrocytes (Westergaard, Sonnewald, & Schousboe, 1995). It is therefore likely that the observed effect on the TCA cycle was due to utilization of the intermediate metabolites, as opposed to production. The switch from TCA cycle metabolism to predominantly glycolytic metabolism would drastically reduce available energy levels in the cell and have an impact on cell survival, which would account for the significant decrease in the number of viable cells after malathion exposure compared to no exposure at 24 hours (Figure 1A). This was also an observed difference in response to permethrin exposure, which had increased levels of TCA cycle intermediates compared to no exposure, and significantly more viable cells present than for malathion exposure at 24 hours.

Interestingly, previous studies on permethrin exposure in rats showed the opposite results to this study and a decrease in TCA cycle intermediates (malate, citrate and 2-oxoglutarate) following exposure to permethrin (Liang et al., 2012, 2013), yet they did not report on glycolytic intermediates, or pyruvate. This suggests that further efforts into the interpretation of the central energy metabolic pathways are hugely important to advance in metabolomics studies. For example, pyruvate is a key molecule that interconnects many metabolic pathways within a cell. Not only important in energy production, being the output of glycolysis and the precursor molecule of the TCA cycle, it can also be converted into carbohydrates, fatty acids and the amino acid, alanine. To be able to interpret further the exact directions that pyruvate follows through the network of pathways within cells, future studies are necessary to explore the response of the metabolome at varying doses to look at the scale of response, as well as several periods of exposure and use of stable isotope-labelled carbon sources (^{13}C–glucose and ^{13}C–glutamine) to investigate metabolic flux (Mueller & Heinzle, 2013; Sims et al., 2013; Wegner, Meiser, Weindl, & Hiller, 2015).

Analysis of the substantial fold changes from the control in the relative abundance of all metabolite features detected uncovered a range of different metabolic responses that were unique to exposure to permethrin or malathion (Figures 4 and S2). A more detailed analysis of these particular metabolite groups in future investigations may provide a clearer picture of the specific biochemical events occurring in the cellular response from exposure to these toxins. One noticeable aspect from the metabolite relative abundance histograms as well as the supporting tables (Tables S1 and S2), is the large margin of error for many of the mean fold changes. These error margins would be improved in future studies by the use of a larger sample size per treatment group, and the use of quality control, pooled samples to correct for the variation in large-scale data sets encountered during metabolomics analyses (Broadhurst & Kell, 2006).

The 'unknown', or unidentified detected features were included in all multivariate statistical analyses and their weighting to the overall metabolic profile of the cells was utilized. Some of these 'unknowns'could be assumed to be artefactual to gas chromatography or the sample preparation processes, and inclusion of blank extraction samples in future analyses would help to clean up this list of unidentified features of potential interest. Despite this, there were substantial fold changes in relative abundance in some of the 'unknown'metabolite features (Figure S2), the scale of which was not seen in any of the putatively identified features both biological and artefactual, and so their potential as compounds of interest was noted. Owing to the large error margins with these higher fold-change features, it is difficult to interpret any such changes, but they help to demonstrate that this metabolomics perspective can detect both high and low relative abundances of a diverse range of different metabolite classes, as a single snap-shot of toxic exposure metabolic response of a cell system. Future investigations should take into consideration the potential for margins of error with single-platform, low sample number studies, and take appropriate action to best fit the experimental design to the variety of data able to be collected.

In this study, the metabolic response was also compared to the observed numbers of viable cells and the appearance of cells in culture (Figures 1 and 2 respectively). Despite a reduction in cell number resulting from exposure to either insecticide, there was a distinct lack of reduction in cell viability (Figure 1). It can be assumed from this that the cell membranes remained intact until immediately before cell death. In the case for future cell culture metabolomics investigations, this cell type appears to be an optimal model for the detection of intracellular metabolites. The analysis of extracellular metabolites from this model may provide a clearer picture of the state of degraded cells that have released their internal metabolites into the surrounding medium. This could further uncover a living cell's metabolic state (Aurich et al., 2015; Nicolae, Wahrheit, Bahnemann, Zeng, & Heinzle, 2014) in the moments immediately preceding cell death, and comparison of this to intracellular metabolites of remaining viable cells may help to interpret where the 'points of no return' might be for the metabolic state of a cell in response to toxins.

5 | CONCLUSIONS

Metabolomics has been proposed as a new and exciting technique to study the toxic effect of environmental chemicals and to test for their safety in mammalian cells. To investigate whether metabolomics can be used to elucidate the metabolic response of the mammalian nervous system to neurotoxic insecticide chemicals, we analysed the metabolome of cultured B50 neuroblastoma cells following exposure to the pyrethroid insecticide permethrin or the organophosphate insecticide malathion. Distinct effects on cell growth and the metabolite profile were observed for both toxic chemicals. This study has

illustrated the ability of metabolomics to detect not only an overall change in the metabolome, but to further identify specific metabolic deviations, which are particularly important for deducing the possible downstream effects on function and stability of the cell, heavily influenced by exposure to a potentially toxic chemical. In this new approach to examination of chemical toxicology, two differing classes of insecticide chemicals, permethrin and malathion, were both found to induce anti-oxidative stress defences, glutamate-mediated excitotoxicity and disturbances in the TCA cycle in cultured neuronal cells.

This study provides proof of concept for future cultured cell metabolomics studies investigating the neurotoxic cellular response to environmental chemicals that may be adversely affecting human health. To elucidate further the finer details of the metabolic processes involved and the potential mechanisms behind the development of disease, this study design should be expanded with multiple doses and varying time points of exposure, which would give a greater understanding of the directional expression of the observed metabolite changes. With the expansion of this metabolomics knowledge of the cellular response to toxins, it may be possible to isolate specific responses to particular toxins, and the downstream effects that can result from chemical exposure, which have currently gone unnoticed and undefined. With more understanding of how chemical exposure has an effect on the metabolism of neuronal cells, it may be possible to define a pathway of disease development demonstrating how environmental chemicals may be implicated in the increasing prevalence of neurological disorders world-wide.

ACKNOWLEDGEMENTS

This work was supported in part by the National Collaborative Research Infrastructure Strategy Bioplatforms Australia, the Australian Government Research Training Program Scholarship, and the McCusker Charitable Foundation.

CONFLICT OF INTEREST

The authors did not report any conflict of interest.

REFERENCES

Abbiss, H., Maker, G. L., Gummer, J., Sharman, M. J., Phillips, J. K., Boyce, M., & Trengove, R. D. (2012). Development of a non-targeted metabolomics method to investigate urine in a rat model of polycystic kidney disease. *Nephrology*, 17, 104–110.

Abbiss, H., Rawlinson, C., Maker, G. L., & Trengove, R. (2015). Assessment of automated trimethylsilyl derivatization protocols for GC-MS-based untargeted metabolomic analysis of urine. *Metabolomics*, 11, 1908–1921.

Abdollahi, M., Ranjbar, A., Shadnia, S., Nikfar, S., & Rezaie, A. (2004). Pesticides and oxidative stress: A review. *Medical Science Monitor*, 10, 141–147. http://www.MedSciMonit.com/pub/vol_10/no_6/4163.pdf

Aliferis, K. A., & Chrysayi-Tokousbalides, M. (2011). Metabolomics in pesticide research and development: Review and future perspectives. *Metabolomics*, 7, 35–53.

Ascherio, A., Chen, H., Weisskopf, M. G., O'Reilly, E., McCullough, M. L., Calle, E. E., … Thun, M. J. (2006). Pesticide exposure and risk for Parkinson's disease. *Annals Neurology*, 60, 197–203.

Aurich, M. K., Paglia, G., Rolfsson, Ó., Hrafnsdóttir, S., Magnúsdóttir, M., Stefaniak, M. M., … Thiele, I. (2015). Prediction of intracellular metabolic states from extracellular metabolomic data. *Metabolomics*, 11, 603–619.

Babina, K., Dollard, M., Pilotto, L., & Edwards, J. W. (2012). Environmental exposure to organophosphorus and pyrethroid pesticides in South Australian preschool children: A cross sectional study. *Environment International*, 48, 109–120.

Banerjee, B. D., Seth, V., & Ahmed, R. S. (2001). Pesticide-induced oxidative stress: Perspectives and trends. *Reviews on Environmental Health*, 16, 1–40.

Becker, K., Seiwert, M., Angerer, J., Kolossa-Gehring, M., Hoppe, H.-W., Ball, M., … Seifert, B. (2006). GerES IV pilot study: Assessment of the exposure of German children to organophosphorus and pyrethroid pesticides. *International Journal of Hygiene and Environmental Health*, 209, 221–233.

Bouchard, M. F., Bellinger, D. C., Wright, R. O., & Weisskopf, M. G. (2010). Attention-deficit/hyperactivity disorder and urinary metabolites of organophosphate residues. *Pediatrics*, 125, 1270–1277.

Bouhifd, M., Hartung, T., Hogberg, H. T., Kleensang, A., & Zhao, L. (2013). Toxicometabolomics. *Journal of Applied Toxicology*, 33, 1365–1383.

Broadhurst, D. I., & Kell, D. B. (2006). Statistical strategies for avoiding false discoveries in metabolomics and related experiments. *Metabolomics*, 2, 171–196.

Choi, D. W. (1988). Glutamate neurotoxicity and diseases of the nervous system. *Neuron*, 1, 623–634.

Curtis, C. F., & Mnzava, A. E. (2000). Comparison of house spraying and insecticide-treated nets for malaria control. *Bulletin of the World Health Organization*, 78, 1389–1400.

Egan, H. (1966). Pesticide residues in fat-containing food and in human fat. *Proceedings of the Nutrition Society*, 25, 44–51.

Ellis, J. K., Athersuch, T. J., Cavill, R., Radford, R., Slattery, C., Jennings, P., … Keun, H. C. (2011). Metabolic response to low-level toxicant exposure in a novel renal tubule epithelial cell system. *Molecular BioSystems*, 7, 247–257.

Fenske, R. A., Lu, C., Barr, D., & Needham, L. (2002). Children's exposure to chlorpyrifos and parathion in an agricultural communitiy in central Washington state. *Environmental Health Perspectives*, 110, 549–553.

Flaskos, J. (2012). The developmental neurotoxicity of organophosphorus insecticides: A direct role for the oxon metabolites. *Toxicology Letters*, 209, 86–93.

Fragar, L. J., Sankaran, B., & Thomas, P. (2005). *Pesticides and Adverse Health Outcomes in Australia*. Barton, ACT: Rural Industries Research and Development Corporation.

Francki, M. G., Hayton, S., Gummer, J. P. A., Rawlinson, C., & Trengove, R. D. (2016). Metabolomic profiling and genomic analysis of wheat aneuploid lines to identify genes controlling biochemical pathways in mature grain. *Plant Biotechnology Journal*, 14, 649–660.

Hemingway, J. (2014). The role of vector control in stopping the transmission of malaria: Threats and opportunities. *Philosophical transactions of the Royal Society of London. Series B, Biological Sciences*, 369, 20130431.

Heudorf, U., Angerer, J., & Drexler, H. (2004). Current internal exposure to pesticides in children and adolescents in Germany: Urinary levels of metabolites of pyrethroid and organophosphorus insecticides. *International Archives of Occupational and Environmental Health*, 77, 67–72.

Huang, S.-M., Zuo, X., Li, J. J. E., Li, S. F. Y., Bay, B. H., & Ong, C. N. (2012). Metabolomics studies show dose-dependent toxicity induced by SiO_2 nanoparticles in MRC-5 human fetal lung fibroblasts. *Advanced Healthcare Materials*, 1, 779–784.

Issam, C., Zohra, H., Monia, Z., & Hassan, B. C. (2011). Effects of dermal subchronic exposure of pubescent rats to permethrin (PRMT) on the histological structures of genital tract, testosterone and lipoperoxidation. *Experimental and Toxicologic Pathology*, 63, 393–400.

Johnson, C. H., Patterson, A. D., Idle, J. R., & Gonzalez, F. J. (2012). Xenobiotic metabolomics: Major impact on the metabolome. *Annual Review of Pharmacology and Toxicology*, 52, 37–56.

Jones, O. A. H., Murfitt, S., Svendsen, C., Turk, A., Turk, H., Spurgeon, D. J., … Griffin, J. L. (2013). Comparisons of metabolic and physiological changes in rats following short term oral dosing with pesticides commonly found in food. *Food and Chemical Toxicology*, 59, 438–445.

Keifer, M. C., & Firestone, J. (2007). Neurotoxicity of pesticides. *Journal of Agromedicine*, 12, 17–25.

Kohlmeier, L., & Kohlmeier, M. (1995). Adipose tissue as a medium for epidemiologic exposure assessment. *Environmental Health Perspectives*, 103, 99–106.

Lee, I., Eriksson, P., Fredriksson, A., Buratovic, S., & Viberg, H. (2015). Developmental neurotoxic effects of two pesticides: Behavior and neuroprotein studies on endosulfan and cypermethrin. *Toxicology*, 335, 1–10.

Liang, Y. J., Wang, H. P., Long, D. X., & Wu, Y. J. (2012). Applying biofluid metabonomic techniques to analyze the combined subchronic toxicity of propoxur and permethrin in rats. *Bioanalysis*, 4, 2897–2907.

Liang, Y. J., Wang, H. P., Long, D. X., Li, W., & Wu, Y. J. (2013). A metabonomic investigation of the effects of 60 days exposure of rats to two types of pyrethroid insecticides. *Chemico-Biological Interactions*, 206, 302–308.

Liu, J., & Schelar, E. (2012). Pesticide exposure and child neurodevelopment: Summary and implications. *Workplace Health & Safety*, 60, 235–242.

Lu, C., Barr, D. B., Pearson, M. A., Walker, L. A., & Bravo, R. (2009). The attribution of urban and suburban children's exposure to synthetic pyrethroid insecticides: A longitudinal assessment. *Journal of Exposure Science and Environmental Epidemiology*, 19, 69–78.

Maroni, M., Colosio, C., Ferioli, A., & Fait, A. (2000). Biological monitoring of pesticide exposure: A review. Introduction. *Toxicology*, 143, 1–118.

Marrs, T. C. (2012). Toxicology of insecticides to mammals. *Pest Management Science*, 68, 1332–1336.

McKenna, M. C. (2007). The glutamate-glutamine cycle is not stoichiometric: Fates of glutamate in brain. *Journal of Neuroscience Research*, 85, 3347–3358.

Mediani, A., Abas, F., Khatib, A., Tan, C. P., Ismail, I. S., Shaari, K., … Lajis, N. H. (2015). Relationship between metabolites composition and biological activities of *Phyllanthus niruri* extracts prepared by different drying methods and solvents extraction. *Plant Foods for Human Nutrition*, 70, 184–192.

Moretto, A., & Colosio, C. (2011). Biochemical and toxicological evidence of neurological effects of pesticides: The example of Parkinson's disease. *Neurotoxicology*, 32, 383–391.

Moser, V. C., Stewart, N., Freeborn, D. L., Crooks, J., MacMillan, D. K., Hedge, J. M., … Herr, D. W. (2015). Assessment of serum biomarkers in rats after exposure to pesticides of different chemical classes. *Toxicology and Applied Pharmacology*, 282, 161–174.

Mueller, D., & Heinzle, E. (2013). Stable isotope-assisted metabolomics to detect metabolic flux changes in mammalian cell cultures. *Current Opinion in Biotechnology*, 24, 54–59.

Naeher, L. P., Tulve, N. S., Egeghy, P. P., Barr, D. B., Adetona, O., Fortmann, R. C., … Sheldon, L. S. (2010). Organophosphorus and pyrethroid insecticide urinary metabolite concentrations in young children living in a southeastern United States city. *Science of the Total Environment*, 408, 1145–1153.

Narahashi, T. (2010). Neurophysiological effects of insecticides. In R. Krieger (Ed.), *Hayes' Handbook of Pesticide Toxicology* (Vol. 1) (pp. 799–817). London: Academic Press.

National Research Council (NRC) (2007). *Toxicity Testing in the 21st Century: A Vision and a Strategy*. Washington DC, USA: National Research Council (NRC).

Ng, J. S., Ryan, U., Trengove, R. D., & Maker, G. L. (2012). Development of an untargeted metabolomics method for the analysis of human faecal samples using cryptosporidium-infected samples. *Molecular and Biochemical Parasitology*, 185, 145–150.

Nicolae, A., Wahrheit, J., Bahnemann, J., Zeng, A.-P., & Heinzle, E. (2014). Non-stationary ^{13}C metabolic flux analysis of Chinese hamster ovary cells in batch culture using extracellular labeling highlights metabolic reversibility and compartmentation. *BMC Systems Biology*, 8, 50–64.

Nishizawa, Y. (2001). Glutamate release and neuronal damage in ischemia. *Life Sciences*, 69, 369–381.

Ojha, A., Yaduvanshi, S. K., Pant, S. C., Lomash, V., & Srivastava, N. (2013). Evaluation of DNA damage and cytotoxicity induced by three commonly used organophosphate pesticides individually and in mixture, in rat tissues. *Environmental Toxicology*, 28, 543–552.

Otey, C. A., Boukhelifa, M., & Maness, P. (2003). B35 neuroblastoma cells: An easily transfected, cultured cell model of central nervous system neurons. *Methods in Cell Biology*, 71, 287–304.

Peng, L., Hertz, L., Huang, R., Sonnewald, U., Petersen, S. B., Westergaard, N., … Schousboe, A. (1993). Utilization of glutamine and of TCA cycle constituents as precursors for transmitter glutamate and GABA. *Developmental Neuroscience*, 15, 367–377.

Purwaha, P., Silva, L. P., Hawke, D. H., Weinstein, J. N., & Lorenzi, P. L. (2014). An artifact in LC-MS/MS measurement of glutamine and glutamic acid: In-source cyclization to pyroglutamic acid. *Analytical Chemistry*, 86, 5633–5637.

Qin, X. Y., Akanuma, H., Wei, F., Nagano, R., Zeng, Q., Imanishi, S., … Sone, H. (2012). Effect of low-dose thalidomide on dopaminergic neuronal differentiation of human neural progenitor cells: A combined study of metabolomics and morphological analysis. *Neurotoxicology*, 33, 1375–1380.

Ramirez, T., Daneshian, M., Kamp, H., Bois, F. Y., Clench, M. R., Coen, M., … Leist, M. (2013). Metabolomics in toxicology and preclinical research. *ALTEX*, 30, 209–225.

Roberts, E. M., English, P. B., Grether, J. K., Windham, G. C., Somberg, L., & Wolf, C. (2007). Maternal residence near agricultural pesticide applicaitons and autism spectrum disorders among children in the California central valley. *Environmental Health Perspectives*, 115, 1482–1489.

Searles Nielson, S., McKean-Cowdin, R., Farin, F. M., Holly, E. A., Preston-Martin, S., & Mueller, B. A. (2010). Childhood brain tumors, residential insecticidal exposure, and pesticide metabolism genes. *Environmental Health Perspectives*, 118, 144–149.

Sévin, D. C., Kuehne, A., Zamboni, N., & Sauer, U. (2015). Biological insights through nontargeted metabolomics. *Current Opinion in Biotechnology*, 34, 1–8.

Sims, J. K., Manteiger, S., & Lee, K. (2013). Towards high resolution analysis of metabolic flux in cells and tissues. *Current Opinion in Biotechnology*, 24, 933–939.

Snouber, L. C., Bunescu, A., Naudot, M., Legallais, C., Brochot, C., Dumas, M. E., … Leclerc, E. (2013). Metabolomics-on-a-chip of hepatotoxicity induced by anticancer drug flutamide and its active metabolite hydroxyflutamide using HepG2/C3a microfluidic biochips. *Toxicological Sciences*, 132, 8–20.

Soderlund, D. M. (2012). Molecular mechanisms of pyrethroid insecticide neurotoxicity: Recent advances. *Archives of Toxicology*, 86, 165–181.

Stenersen, J. (2004). *Chemical Pesticides: Mode of Action and Toxicology*. Florida: CRC Press.

Tian, C., Sun, L., Jia, B., Ma, K., Curthoys, N., Ding, J., & Zheng, J. (2012). Mitochondrial glutaminase release contributes to glutamate-mediated neurotoxicity during human immunodeficiency virus-1 infection. *Journal of Neuroimmune Pharmacology*, 7, 619–628.

Timofeeva, O. A., & Levin, E. D. (2010). Lasting behavioural consequences of organophosphate pesticide exposure during development. In R. Krieger (Ed.), *Hayes' Handbook of Pesticide Toxicology* (Vol. 1) (pp. 837–846). London: Academic Press.

Van den Hof, W. F. P. M., Ruiz-Aracama, A., Van Summeren, A., Jennen, D. G. J., Gaj, S., Coonen, M. L. J., … Kleinjans, J. C. S. (2015). Integrating multiple omics to unravel mechanisms of cyclosporin a induced hepatotoxicity *in vitro*. *Toxicology In Vitro*, 29, 489–501.

Veyrat-Durebex, C., Corcia, P., Piver, E., Devos, D., Dangoumau, A., Gouel, F., … Blasco, H. (2016). Disruption of TCA cycle and glutamate metabolism identified by metabolomics in an *in vitro* model of amyotrophic lateral sclerosis. *Molecular Neurobiology*, 53, 6910–6924.

van Vliet, E., Morath, S., Eskes, C., Linge, J., Rappsilber, J., Honegger, P., … Coecke, S. (2008). A novel *in vitro* metabolomics approach for neurotoxicity testing, proof of principle for methyl mercury chloride and caffeine. *Neurotoxicology*, 29, 1–12.

Wang, Y., & Qiu, Z. H. (2010). Molecular and cellular mechanisms of excitotoxic neuronal death. *Apoptosis*, 15, 1382–1402.

Ward, M. W., Rego, A. C., Frenguelli, B. G., & Nicholls, D. G. (2000). Mitochondrial membrane potential and glutamate excitotoxicity in cultured cerebellar granule cells. *Journal of Neuroscience*, 20, 7208–7219.

Wegner, A., Meiser, J., Weindl, D., & Hiller, K. (2015). How metabolites modulate metabolic flux. *Current Opinion in Biotechnology*, 34, 16–22.

Welsh-Bohmer, K. A., Plassman, B. L., & Hayden, K. M. (2010). Genetic and envrionmental contributions to cognitive decline in aging and Alzheimer's disease. *Annual Review of Gerontology & Geriatrics*, 30, 81–114.

Wenner, M. I., Maker, G. L., Dawson, L. F., Drummond, P. D., & Mullaney, I. (2016). The potential of metabolomic analysis techniques for the characterisation of α1-adrenergic receptors in cultured N1E-115 mouse neuroblastoma cells. *Cytotechnology*, 68, 1561–1575.

Westergaard, N., Sonnewald, U., & Schousboe, A. (1995). Metabolic trafficking between neurons and astrocytes: The glutamate/glutamine cycle revisited. *Developmental Neuroscience*, 17, 203–211.

Zaganas, I., Kapetanaki, S., Mastorodemos, V., Kanavouras, K., Colosio, C., Wilks, M. F., & Tsatsakis, A. M. (2013). Linking pesticide exposure and dementia: What is the evidence? *Toxicology*, 307, 3–11.

Zurich, M. G., & Monnet-Tschudi, F. (2009). Contribution of *in vitro* neurotoxicology studies to the elucidation of neurodegenerative processes. *Brain Research Bulletin*, 80, 211–216.

SUPPORTING INFORMATION

Additional Supporting Information may be found online in the supporting information tab for this article.

How to cite this article: Hayton S, Maker GL, Mullaney I, Trengove RD. Untargeted metabolomics of neuronal cell culture: A model system for the toxicity testing of insecticide chemical exposure. *J Appl Toxicol*. 2017;37:1481–1492. https://doi.org/10.1002/jat.3498